this issue in the present study. Increased oxidative stress in the RVLM does contribute to the hypertensive mechanisms of SHRSP (14).

We microinjected selective antagonists of iNOS, aminoguanidine, and AMT, directly into the RVLM and did not observe changes in BP or HR in normotensive WKY. In contrast, microinjection of aminoguanidine into the RVLM elicits a pressor and tachycardic response in Sprague-Dawley rats anesthetized with propofol (15). Similar doses of aminoguanidine were used in the present study. In addition, microinjection of lipopolysaccharides into the RVLM reduces BP and HR in WKY and SHR, although the magnitude of the effect is significantly greater in WKY than in SHR (16). Co-administration of the selective iNOS inhibitor, S-methylisothiourea, significantly attenuates the effects of the lipopolysaccharide injection, suggesting that the hypotensive and bradycardic responses are mediated by iNOS (16). In the present study, however, microinjection of iNOS inhibitors into the RVLM induced a depressor response. We do not have a clear explanation for the discrepancy between our observation and that of Chan, Wang, Wu, and Chan, because they did not report the effects of microinjection of iNOS inhibitors alone into the RVLM between WKY and SHR. It is possible that microinjection of lipopolysaccarides into the RVLM is harmful and therefore induces other cytokines that might cause hypotension, bradycardia, and death (16). It is also possible that the increased reactive oxygen species, which interact with NO in the RVLM, contribute to hypertensive mechanisms in SHR (14). Consistent with this notion, microinjection of a membrane-permeable superoxide mimetic into the RVLM normalizes blood pressure in SHR to the level of WKY (17). In fact, microinjection of tempol into the RVLM decreases blood pressure in rats with iNOS overexpression in the RVLM (14), further supporting this notion.

Changes in the levels of NO production and reactive oxygen species in the brain, which are affected by oral treatment with anti-hypertensive drugs, such as calcium channel blockers, regulate BP (18,19). An angiotensin receptor blocker might have the same effect on reactive oxygen species (20) induced in part by iNOS. Further studies are necessary to examine which drugs have these beneficial effects in hypertensive patients. In conclusion, the present study suggests that the increased iNOS expression in the RVLM contributes to hypertension in SHR.

Acknowledgments

This study was supported by a Grant-in-Aid for Scientific Research from the Japan Promotion of Science and, in part, by the Health and Labor Sciences Research Grant for Comprehensive Research in Aging and Health Labor and Welfare of Japan.

Declaration of Interest

The authors report no conflicts of interest. The authors alone are responsible for the content and writing of the paper.

References

1. Patel KP, Li Y-F, Hirooka Y. Role of nitric oxide in central sympathetic outflow. *Exp Biol Med* 2001;226:814–824.
2. Zanzinger J. Role of nitric oxide in the neural control of cardiovascular function. *Cardiovasc Res* 1999;43:639–649.

3. Guyenet PG. The sympathetic control of blood pressure. *Nat Rev Neurosci* 2006;7:335–346.
4. Dampney RAL. Functional organization of central pathways regulating the cardiovascular system. *Physiol Rev* 1994;74:323–364.
5. Chou T-C, Yen M-H, Li C-Y, Ding Y-A. Alteration of nitric oxide synthase expression with aging and hypertension in rats. *Hypertension* 1998;31:643–648.
6. Yamakawa H, Jerova M, Ando H, Saavedra JM. Normalization of endothelial and inducible nitric oxide synthase expression in brain microvessels of spontaneously hypertensive rats by angiotensin II AT1 receptor inhibition. *J Cereb Blood Flow Metab* 2003;23:371–380.
7. Sesso HD, Buring JE, Rifai N, Blake GJ, Gaziano JM, Ridker PM. C-reactive protein and the risk of developing hypertension. *JAMA* 2003;290:2945–2951.
8. Pedrinelli R, Dell'Omo G, Di Bello V, Pellegrini G, Pucci L, Del Prato S, Penno G. Low-grade inflammation and microalbuminuria in hypertension. *Arterioscler Thromb Vasc Biol* 2004;24:2414–2419.
9. Salles GF, Fiszman R, Cardoso CRL, Muxfeldt ES. Relation of left ventricular hypertrophy with systemic inflammation and endothelial damage in resistant hypertension. *Hypertension* 2007;50:723–728.
10. Kimura Y, Hirooka Y, Sagara Y, Ito K, Kishi T, Shimokawa H, Takeshita A, Sunagawa K. Overexpression of inducible nitric oxide synthase in rostral ventrolateral medulla causes hypertension and sympathoexcitation via an increase in oxidative stress. *Circ Res* 2005;96:252–260.
11. Hirooka Y, Shigematsu H, Kishi T, Kimua Y, Ueta Y, Takeshita A. Reduced nitric oxide synthase in the brainstem contributes to enhanced sympathetic drive in rats with heart failure. *J Cardiovasc Pharmacol* 2003;42(suppl. 1):S111–S115.
12. Kishi T, Hirooka Y, Ito K, Sakai K, Shimokawa H, Takeshita A. Cardiovascular effects of overexpression of endothelial nitric oxide synthase in the rostral ventrolateral medulla in stroke-prone spontaneously hypertensive rats. *Hypertension* 2002;39:264–268.
13. Kishi T, Hirooka Y, Mukai Y, Shimokawa H, Takeshita A. Atorvastatin causes depressor and sympatho-inhibitory effects with upregulation of nitric synthases in stroke-prone spontaneously hypertensive rats. *J Hypertens* 2003;21:379–386.
14. Kishi T, Hirooka Y, Kimura Y, Ito K, Shimokawa H, Takeshita A. Increased reactive oxygen species in rostral ventrolateral medulla contribute to neural mechanisms of hypertension in stroke-prone spontaneously hypertensive rats. *Circulation* 2004;109:2357–2362.
15. Chan SHH, Wang L-L, Wang S-H, Chan JYH. Differential cardiovascular responses to blockade of nNOS or iNOS in rostral ventrolateral medulla of the rat. *Br J Pharmacol* 2001;133:606–614.
16. Chan JYH, Wang L-L, Wu KLH, Chan SHH. Reduced functional expression and molecular synthesis of inducible nitric oxide synthase in rostral ventrolateral medulla of spontaneously hypertensive rats. *Circulation* 2001;104:1676–1681.
17. Tai M-H, Wang L-L, Wu KLH, Chan JYH. Increased superoxide anion in rostral ventrolateral medulla contributes to hypertension in spontaneously hypertensive rats via interactions with nitric oxide. *Free Rad Biol Med* 2005;38:450–462.
18. Kimura Y, Hirooka Y, Sagara Y, Sunagawa K. Long-acting calcium channel blocker, azelnidipine, increases endothelial nitric oxide synthase in the brain and inhibits sympathetic nerve activity. *Clin Exp Hypertens* 2007;29:13–21.
19. Hirooka Y, Kimura Y, Nozoe M, Sagara Y, Ito K, Sunagawa K. Amlodipine-induced reduction of oxidative stress in the brain is associated with sympatho-inhibitory effects in stroke-prone spontaneously hypertensive rats. *Hypertens Res* 2006;29:49–56.
20. Sagara Y, Ito L, Kimura Y, Hirooka Y. Telmisartan reduces oxidative stress in the brain with sympathoinhibitory effects in stroke-prone spontaneously hypertensive rats. *Circulation* 2004;110 (suppl. III): 265 (abstract).

Clinical and Experimental Hypertension, 31:241–249, 2009

ISSN: 1064-1963 print / 1525-6006 online
DOI: 10.1080/10641960902822492

informa
healthcare

Cilnidipine Inhibits the Sympathetic Nerve Activity and Improves Baroreflex Sensitivity in Patients with Hypertension

TAKUYA KISHI, YOSHITAKA HIROOKA, SATOMI KONNO, AND KENJI SUNAGAWA

Department of Cardiovascular Medicine, Kyushu University, Graduate School of Medical Sciences, Fukuoka, Japan

N-type calcium channel blocker, cilnidipine, is reported not to increase the heart rate in spite of the strong depressor effect. However, it has not been determined whether cilnidipine has the sympatho-inhibitory effects or not. Moreover, the effect of cilnidipine on the baroreflex control has not been determined. The aim of this study was to determine the effect of cilnidipine on sympathetic and parasympathetic nerve activity, and baroreflex sensitivity. We studied five hypertensive patients treated with 10 mg cilnidipine (10-mg group) and five hypertensive patients treated with 20 mg cilnidipine (20-mg group). Before the treatment and 6 months after the treatment, we measured the blood pressure, spontaneous baroreflex sensitivity (BRS), heart rate variability (HRV), and blood pressure variability (BPV). After 6 months, systolic blood pressure (SBP) and the low-frequency component of systolic BPV expressed in normalized units (LFnuSBP), as the parameter of sympathetic nerve activity, was significantly decreased in both groups, and the suppressive effects were stronger in the 20-mg group than in the 10-mg group. The high-frequency component of HRV expressed in normalized units, as the parameter of parasympathetic nerve activity, and BRS were significantly increased in 20-mg group, but not significant in 10-mg group. These results suggest that 6 months treatment with cilnidipine for hypertension has the sympatho-inhibtory effect, and that high-dose cilnidipine improves the parasympathetic nerve activity and baroreflex control in patients with hypertension.

Keywords N-type calcium channels blocker, hypertension, sympathetic nerve activity, baroreflex sensitivity

Introduction

Hypertension is an established risk factor in the prognosis of cardiovascular diseases and organ damage. It may be feasible for patients with hypertension or at high cardiovascular risk to receive a blood pressure-lowering medication in order to achieve a

Submitted September 3, 2007; revised January 17, 2008; accepted April 24, 2008.
Address correspondence to Takuya Kishi, MD, PhD, Department of Cardiovascular Medicine, Kyushu University, Graduate School of Medical Sciences, 3-1-1 Maidashi, Higashi-ku, Fukuoka 812-8582, Japan; E-mail: tkishi@cardiol.med.kyushu-u.ac.jp

reduction of stroke and cardiovascular complications (1). Ca channel blocker is widely used as the blood pressure-lowering agents. However, it has been reported that Ca channels blocker increases heart rate with lowering blood pressure. Among the Ca channels blockers, cilnidipine is known not to increase the heart rate and plasma norepinehrine concentrations in spite of the strong blood pressure lowering effects (2–4). Cilnidipine is a long-acting dihydropyridine calcium channel blocker by inhibiting L-type calcium channels directly associated with vascular tone, and N-type calcium channels related to sympathetic nervous activity (5–7). Whereas cilnidipine inhibits N-type calcium channels, it has not been well established whether cilnidipine decreases the sympathetic nerve activity and increases the parasympathetic nerve activity in the patients with hypertension.

Analysis of spontaneous heart rate and blood pressure variability offers insights into different features of autonomic control of circulation (8), including the arterial baroreflex regulation (9). In this context, heart rate spectral powers in the so-called high-frequency (HF; 0.15–0.40 Hz) and low-frequency (LF; 0.04–0.15 Hz) regions and blood pressure spectra powers in the LF regions have been repeatedly reported to provide relevant information (8, 10–12). The LF power of blood pressure was reported to be increased in parallel with the sympathetic nerve activation (13). Furthermore, the baroreflex control is one of the key mechanisms responsible for the short-term control of blood pressure. Impairment of this reflex has been found in a number of conditions, such as aging (14), heart failure (15), post-myocardial infarction (16), and the impairment of baroreflex sensitivity (BRS) is known as the predictive factor of mortality in hypertension (17). Baroreflex sensitivity was originally assessed by intra-arterial measurement of the change in pulse interval following a pharmacologically induced change in blood pressure. However, for some time now, noninvasive monitoring of blood pressure using finger plethysmography has been available (18), and is an accepted method for tracking beat-to-beat changes in blood pressure (19). Added to this, a further method for measuring BRS has been developed, which assesses spontaneous changes in blood pressure and pulse interval, and does not require pharmacological manipulation of blood pressure-spectral analysis (20,21). However, it has not been determined whether the cilnidipine improves the impaired BRS or not.

Therefore, the aim of the present study was to evaluate the effect of cilnidipine on the sympathetic nerve activity, parasympathetic nerve activity, and BRS in the patients with hypertension. We evaluated the sympathetic and parasympathetic nerve activity using the analysis of systolic blood pressure and heart rate variability, and BRS was measured by the spontaneous sequence method.

Materials and Methods

Subjects

The present study was conducted prospectively on 10 outpatients with hypertension (5 males and 5 females; mean age: 58.6 years; range 44–74 years) whose blood pressure was over 140/90 mmHg. No patients were currently receiving anti-hypertensive medication and all of them were newly diagnosed. Patients with the secondary hypertension were excluded. All studies were performed between 9 and 11 a.m., with each subject examined at the same time of day on each visit to reduce the possible influence of circadian variation in BRS. This study was performed in a quiet room, and every effort was made to keep stimuli to a minimum during the study period. Each subject gave informed

consent to the experimental procedures, which was approved by the ethics committee of our institution.

Measurement of Blood Pressure and Heart Rate

Subjects lay supine, and were rested for a minimum of 15 minutes prior to assessment. Each subject then underwent periods of blood pressure and heart rate monitoring. Blood pressure monitoring was performed using the TaskForce Monitor 3040i (CNSystems, Graz, Austria). The cuff was attached to a finger of the left hand and supported at heart level. Electrocardiogram electrodes were attached to the chest. After a minimum period of 5 minutes, and once a reading of blood pressure and heart rate had stabilized, three consecutive, 5-minute recordings were made of the blood pressure and electrocardiogram tracing. Noninvasive brachial blood pressure readings were taken with an appropriate-sized cuff.

Spectral Analysis for Systolic Blood Pressure and Heart Rate

Spectral analysis was performed using an adaptive auto-regressive model to provide power spectra for both systolic blood pressure (SBP) and R-R interval (RRI). Low Frequency power of SBP was computed by integrating the spectra between 0.04 and 0.15 Hz, and HF power of RRI was computed by integrating the spectra between 0.15–0.40 Hz. Parasympathetic nerve activity was represented by the normalized unit of HF component of RRI (HFnuRRI), and sympathetic nerve activity was represented by the normalized unit of LF component of SBP (LFnuSBP).

Measurement of Baroreflex Sensitivity by Spontaneous Sequence Method

Sequence analysis detected sequences of three or more beats in which there was either an increase in SBP and pulse interval (Up sequence) or a decrease in SBP and pulse interval (Down sequence). Baroreflex sensitivity was estimated as the mean slope of the up sequences (UP BRS), the down sequences (Down BRS), and also the mean slope of all sequences (Sequence BRS) (20,21). Previous reports showed that this protocol measures BRS accurately in animals compared to standard pharmacological techniques (20,21).

Administration of Cilnidipine

Cilnidipine was administered at a dosage of 10–20 mg (10-mg group and 20-mg group) once daily after breakfast according to the guidelines of the treatment with hypertension of the Japanese Society of Hypertension (JSH2004). All the patients were placed on monotherapy with cilnidipine.

Statistical Analysis

All values were expressed as the mean ± SEM. The student's paired *t*-test was used to analyze the changes of variables between pre- and post-treatment with cilnidipine. Differences in variables between the groups were analyzed by one-way ANOVA. A value of $p < 0.05$ was considered statistically significant.

Results

Patients Characteristics

Table 1 shows the baseline characteristics of the two groups. There were no significant differences in age, blood pressure, serum creatinine, and hemoglobin between 10-mg and 20-mg group of cilnidipine. None of the patients had the clinical side effects of cilnidipine.

Effects of Cilnidipine on Blood Pressure and Heart Rate

After the treatment with cilnidipine for 6 months, blood pressure was significantly reduced in all patients, and the effect of blood pressure lowering was significantly greater in 20-mg group than in 10-mg group (Tables 2, 3, and 4). Heart rate was not significantly decreased in both groups after the treatment with cilnidipine (Tables 2, 3, 4).

Effects of Cilnidipine on Sympathetic and Parasympathetic Nerve Activity

After the treatment with cilnidipine for 6 months, LFnuSBP were significantly decreased in both groups (Tables 2 and 3), and the suppressive effects were stronger in the 20-mg group than in the 10-mg group (Table 4). While HFnuRRI was not significantly changed in the 10-mg group (Table 2), it was significantly increased in the 20-mg group (Table 3).

Effects of Cilnidipine on Baroreflex Sensitivity

In the 10-mg group, BRS was not significantly changed between before and after the treatment with cilnidipine (Table 2). However, in the 20-mg group, BRS was significantly improved after the treatment with cilnidipine for 6 months (Table 3).

Table 1
Clinical profile of the patients in 10-mg and 20-mg group

	10-mg Group (n = 5)	20-mg Group (n = 5)	
Age (year)	56 ± 7	59 ± 8	NS
Systolic blood pressure (mmHg)	161 ± 13	157 ±12	NS
Diastolic blood pressure (mmHg)	100 ± 5	98 ± 8	NS
Heart rate (bpm)	80 ± 5	76 ± 6	NS
AST/ALT (IU/L)	26 ± 11/27 ± 13	26 ± 9/28 ± 6	NS
Cr (mg/dL)	0.7 ± 0.2	0.8 ± 0.2	NS
Total cholesterol (mg/dL)	182 ±19	178 ± 22	NS
Triglyceride (mg/dL)	92 ± 33	88 ± 36	NS
LDL cholesterol (mg/dL)	110 ± 14	108 ± 12	NS
HDL cholesterol (mg/dL)	46 ± 7	48 ± 6	NS
Glucose (mg/dL)	89 ± 11	93 ± 10	NS
HbA1c (%)	5.6 ± 0.4	5.5 ± 0.6	NS
BNP (pg/ml)	38 ± 14	32 ± 11	NS
Left ventricular ejection fraction (%)	70 ± 9	72 ± 8	NS
Cardio-thoracic ratio(%)	54 ± 8	51 ± 8	NS

Table 2
Changes in blood pressure, heart rate, and autonomic function in the patients with 10-mg group

	Pretreatment (n = 5)	Cilnidipine 10 mg (n = 5)	P
Systolic blood pressure (mmHg)	161 ± 13	137 ± 13	< 0.05
Diastolic blood pressure (mmHg)	100 ± 5	87 ± 4	< 0.05
Heart rate (bpm)	80 ± 5	76 ± 7	NS
HF-RR (ms2)	102 ± 63	106 ± 58	NS
HFnuRR (%)	39 ± 6	42 ± 6	NS
LF-SBP (mmHg2)	0.7 ± 0.3	0.5 ± 0.5	NS
LFnuSBP (%)	56 ± 5	49 ± 4	< 0.05
Baroreflex sensitivity (ms/mmHg)	14.2 ± 2.6	16.2 ± 4.8	NS

Table 3
Changes in blood pressure, heart rate, and autonomic function in the patients with 20-mg group

	Pretreatment (n = 5)	Cilnidipine 20 mg (n = 5)	P
Systolic blood pressure (mmHg)	157 ± 12	120 ± 13	< 0.05
Diastolic blood pressure (mmHg)	98 ± 8	81 ± 5	< 0.05
Heart rate (bpm)	76 ± 6	73 ± 6	NS
HF-RR (ms2)	92 ± 44	102 ± 66	NS
HFnuRR (%)	39 ± 3	44 ± 2	< 0.05
LF-SBP (mmHg2)	0.6 ± 0.4	0.4 ± 0.3	NS
LFnuSBP (%)	63 ± 6	50 ± 4	< 0.05
Baroreflex sensitivity (ms/mmHg)	13.6 ± 2.9	20.2 ± 2.1	< 0.05

Table 4
Degree of changes in blood pressure, heart rate and autonomic function in the patients with 10-mg and 20-mg group

	Cilnidipine 10 mg (n = 5)	Cilnidipine 20 mg (n = 5)	P
Systolic blood pressure	−15%	−24%	< 0.05
Diastolic blood pressure	−13%	−17%	< 0.05
Heart rate	−5%	−4%	NS
HFnuRR	+7%	+13%	< 0.05
LFnuSBP	−12%	−12%	< 0.05
Baroreflex sensitivity	+14%	+49%	< 0.05

Discussion

In the present study conducted among patients with essential hypertension, cilnidipine produced a significant reduction in blood pressure with the inhibition of sympathetic nerve activity and the improvement of impaired baroreflex control. This study was the first to report that cilnidipine treatment achieved the inhibition of sympathetic nerve activity and the improvement of the impaired baroreflex control in the patients with hypertension. These results suggest that cilnidipine is preferable for the treatment with hypertension among the Ca channel blockers.

Epidemiological studies have demonstrated that a higher heart rate is associated with a long-term risk of cardiovascular mortality, independent of other cardiac risk factors (22). Therefore, anti-hypertensive drugs that do not increase the heart rate would seem to be preferable. It has been reported that the treatment with short-acting Ca channel blockers may not prevent cardiovascular disease (23,24). Accordingly, long-lasting Ca channel blockers that exert less influence on the sympathetic nervous system are now recommended for the treatment of hypertension. Amlodipine and cilnidipine, which were known as long-acting Ca channel blockers, were reported not to increase heart rate. Eguchi et al. (27) reported that cilnidipine did not cause reflex tachycardia, and that cilnidipine, but not amlodipine, significantly decreased the ambulatory BP level without causing an increase in heart rate. In this study, cilnidipine did not increase heart rate, and caused a significant decrease in the LFnuSBP, as the marker of the sympathetic nerve activity. Our results of the sympatho-inhibitory effects of cilnidipine were similar to the previous reports which calculated the sympathetic nerve activity by other methods. From these results, cilnidipine is considered to be the preferable drug with the sympatho-inhibtory effect among the Ca channel blockers.

In this study, BRS was improved in the patients with hypertension treated with high-dose cilnidipine. A previous study reported that BRS values calculated by sequence analysis had reasonable reproducibility when up and down sequences were combined (25), and we measured the BRS by sequence analysis. It has been reported that BRS is impaired in the patients with hypertension (17,26–29), and that BRS is the predictive factor of mortality and cardiovascular events (17). The results of this study suggest that cilnidipine is preferable for the treatment of hypertension among the Ca channel blockers. Previous studies suggested BRS measured by the sequence method was impaired in the patients with hypertension (5–12 ms/mmHg) (27–29), and BRS obtained in this study was considered to be higher compared to that in those previous studies. This difference may be due to the patients' characteristics in this study. The patients in this study had no complications and their hypertension was in early stages.

The mechanisms in which cilnidipine inhibits the sympathetic nerve activity may be due to suppressing the release of catecholamines from sympathetic nerve endings by blocking the N-type calcium channels distributed widely in sympathetic nerves (30). Recent studies have demonstrated the beneficial effect of cilnidipine on cardiac sympathetic nerve activity and cardiovascular morbidity (31–33). Sakata, Yoshida, and Obayashi reported that cilnidipine suppressed cardiac sympathetic overactivity while amlodipine had little suppressive effect (32). The effect of cilnidipine on heart rate might be due to not only long-acting effects but also to a reduction in sympathetic nerve activity. The mechanisms in which cilnidipine improved the BRS has not been determined in this study. Our previous study in animal models indicated that sympatho-inhibition causes the improvement of BRS in hypertensive model rats (26). Further clinical studies are necessary.

There are several limitations in this study. First, this study was a small-size, nonrandomized study. To establish the sympatho-inhibitory effect and improvement of BRS of cilnidipine, a randomized study is required. Second, the ages of the patients in this study were relatively young, and none of them had organ damage due to hypertension. Whether the treatment with cilnidipine causes the beneficial effects in this study in the older and complicated patients with hypertension has not been determined. Third, we determined the effects of cilnidipine on autonomic function for only 6 months, and only at two points, before and after 6 months. The blood pressure-lowering effect of cilnidipine is determined in several days after the initiation of administration (3). In the present study, we examined the effects of cilnidipine on the autonomic function at only two points pre—administration and after 6 months. From the results of the present study, we have not determined whether the mechanisms of the action of cilnidipine is similar between several days and 6 months after the initiation of cilnidipine. Furthermore, the effects of cilnidipine on the autonomic function for longer periods must be determined.

Conclusion

The treatment with cilnidipine for essential hypertension produced a significant reduction in blood pressure with the inhibition of sympathetic nerve activity and the improvement of impaired baroreflex control. These results suggest that cilnidipine is preferable for the treatment of hypertension among the Ca channel blockers.

Acknowledgments

This work was supported by a Grant-in-Aid for Scientific Research from the Japan Society for the Promotion of Science (B19390231), and in part, by the Health and Labor Sciences Research Grant for Comprehensive Research in Aging and Health Labor and Welfare of Japan. We thank all medical staff of the Department of Cardiovascular Medicine of Kyushu University Hospital, our colleagues, friends, parents, and special thanks to my co-author, Dr. Satomi Konno.

Declaration of Interest

The authors report no conflicts of interest. The authors alone are responsible for the content and writing of the paper.

References

1. Staessen JA, Wang JG, Thijs L. Cardiovascular prevention and blood pressure reduction: a quantitative overview updated until March 2003. *J Hypertens.* 2003;21:1055–1076.
2. Yoshimoto R, Hashiguchi Y, Dohmoto H, Hosono M, Iida H, Fujiyoshi T, Ikeda K, Hayashi Y. Effects of a new dihydropyridine derivative, FRC-8653, on blood pressure in conscious spontaneously hypertensive rats. *J Pharmacobio Dyn* 1992;15:25–32.
3. Tominaga M, Phya Y, Tsukashima A, Kobayashi K, Takata Y, Koga T, Yamashita Y, Fujishima Y, Fujishima M. Ambulatory blood pressure monitoring in patients with essential hypertension treated with a new calcium antagonist, cilnidipine. *Cardiovasc Drugs Ther* 1997;11:43–48.
4. Hosono M, Fujii S, Hiruma T, Watanabe K, Hayashi Y, Ohnishi H, Takata Y, Kato H. Inhibitory effect of cilnidipine on vascular sympathetic neurotransmission and subsequent vasoconstriction in spontaneously hypertensive rats. *Jpn J Pharmacol* 1995;69:127–134.

5. Oike M, Inoue Y, Kitamura K, Kuriyama H. Dual action of FRC8653, a novel dihydropyridine derivative, on the Ba2+ current recorded from the rabbit artery. *Circ Res* 1990;57:993–1006.
6. Fujii S, Kameyama K, Hosono M, Hayashi Y, Kitamura K. Effect of cilnidipine, a new dihidropyrydine Ca++ channel antagonist, on N-type Ca++ channel in rat dorsal root ganglion neurons. *J Pharmacol Exp Ther* 1997;280:1184–1191.
7. Uneyama H, Takahara A, Dohmoto H, Yoshimoto R, Inoue K, Akaike N. Blockade of N-type Ca++ current by cilnidipine (FRC-8653) in acutely dissociated rat sympathetic neurons. *Br J Pharmacol* 1997;122:37–42.
8. Mancia G, Parati G, Castiglioni P, Di Rienzo M. Effect of sinoaortic devervation on frequency-domain estimates of baroreflex sensitivity in conscious cats. *Am J Physiol* 1999;276:H1987–H1993.
9. Laude D, Elghozi JL, Girard A, Bellard E, Bouhaddi M, Castiglioni P, Cerutti C, Cividjian A, Di Rienzo M, Fortrat JO, Janssen B, Karemaker JM, Leftheriotis G, Parati G, Persson PB, Porta A, Quintin L, Regnard J, Rudiger H, Stauss HM. Comparison of various techniques used to estimate spontaneous baroreflex sensitivity. *Am J Physiol* 2004;286:R226–R231.
10. Task Force of the European Society of Cardiology and the North American Society of Pacing and Electrophysiology. Heart rate variability: standards of measurement, physiological interpretation, and clinical ise. *Eur Heart J* 1996;17:354–381.
11. Lucini D, Meta GS, Malliani A, Pagani M. Impairment in cardiac autonomic regulation preceding arterial hypertension in humans: insights from spectral analysis of beat-by-beat cardiovascular variability. *Circulation* 2002;106:2673–2679.
12. Radaelli A, Perlangeli S, Cerutti MC, Mircoli L, Mori I, Boselli K, Bonaita M, Terzoli L, Candotti G, SIgnorini G, Ferrari AU. Altered blood pressure variability in patients with congestive heart failure. *J Hypertens* 1999;17:1905–1910.
13. Castiglioni P, Di Rienzo M, Veicsteinas A, Parati G, Merati G. Mechanisms of blood pressure and heart rate variability: an insight from low-level paraplegia. *Am J Physiol* 2007;292: R1502–R1509.
14. Latinen T, Hartikainen J, Vanninen E, Niskanen L, Geelen G, Lansimies E. Age and gender dependency of baroreflex sensitivity in healthy subjects. *J Appl Physiol* 1998;84:576–583.
15. Mortara A, La Rovere MT, Pinna GD, Prpa A, Maestri R, Fedo O, Pozzoli M, Opasich C, Tavazzi L. Arterial baroreflex modulation of heart rate in chronic heart failure: clinical and hemodynamic correlates and prognostic implications. *Circulation* 1997;96:3450–3458.
16. Farrell TG, Odemuyiwa O, Bashir Y, Gripps TR, Malik M, Ward DE, Camm AJ. Prognostic value of baroreflex sensitivity testing after acute myocardial infarction. *Br Heart J* 1992;67: 129–137.
17. Hesse C, Charkoudian N, Liu Z, Joyner MJ, Eisenach JH. Baroreflex sensitivity inversely correlates with ambulatory blood pressure in healthy normotensive humans. *Hypertension* 2007;50: 41–46.
18. Imholz BP, Wielong W, Langewouters GJ, van Montfrans GA. Continuous finger arterial pressure: utility in the cardiovascular laboratory. *Clin Auton Res* 1991;l1:43–53.
19. Imholz BP, Wieling W, van Montfrans GA, Wesseling KH. Fifteen years experience with finger arterial pressure monitoring: assessment of the technology. *Cardiovasc Res* 1998;38:605–616.
20. Waki H, Kasparov S, Wong LF, Murphy D, Shimizu T, Paton JFR. Chronic inhibition of eNOS activity in nucleus tractus solitarii enhances baroreceptor reflex in conscious rats. *J Physiol* 2003;546:233–242.
21. Waki H, Katahira K, Polson JW, Kasparov S, Murphy D, Paton JFR. Automation of analysis of cardiovascular autonomic function from chronic measurements of arterial pressure in conscious rats. *Exp Physiol*. 2006;91:201–213.
22. Gillman MW, Kannel WB, Belanger A, D'Agostuno RB. Influence of heart rate on mortality among patients with hypertension: the Framingham Study. *Am Heart J* 1993;125:1148–1154.
23. Furberg CD, Psaty BM, Meyer JV. Nifedipine: Dose-related increase in mortality in patients with coronary heart disease. *Circulation* 1995;92:1326–1331.
24. Psaty BM, Heckbert SR, Koepsell TD. The risk of myocardial infarction associated with antihypertensive drug therapies. *JAMA* 1995;274:620–625.

25. Johnson P, Shore A, Potter J, Panerai R, James M. Baroreflex sensitivity measured by spectral and sequence analysis in cerebrovascular disease. *Clin Auton Res* 2006;16:270–275.
26. Kishi T, Hirooka Y, Kimura Y, Sakai K, Ito K, Shimokawa H, Takeshita A. Overexpression of eNOS in RVLM improves impaired baroreflex control of heart rate in SHRSP. *Hypertension* 2003;41:255–260.
27. Eguchi K, Tomizawa H, Ishikawa J, Hoshide S, Pickering TG, Shimada K, Kario K. Factors associated with baroreflex sensitivity: associated with morning blood pressure. *Hypertens Res* 2007;30:723–728.
28. Milan A, Caserta MA, Del Colle S, Dematteis A, Morello F, Rabbia F, Mulatero P, Pandian NG, Veglio F. Baroreflex sensitivity correlates with left ventricular morphology and diastolic function in essential hypertension. *J Hypertens* 2007;25:1655–1664.
29. Eguchi K, Tomizawa H, Ishikawa J, Hoshide S, Fukuda T, Numao T, Shimada K, Kario K. Effects of new calcium channel blocker, azelnidipine, and amlodipine on baroreflex sensitivity and ambulatory blood pressure. *J Cardiovasc Pharmacol* 2007;49:394–400.
30. Yamagishi T. Beneficial effect of cilnidipine on morning hypertension and white-coat effect in patients with essential hypertension. *Hypertens Res* 2006;29:339–344.
31. Sakaki T, Naruse H, Masai M. Cilnidipine as an agent to lower blood pressure without sympathetic nervous activation as demonstrated by iodine-123 metaiodobenzyl guanidine imaging in rat heart. *Ann Nucl Med* 2003;17:321–326.
32. Sakata K, Yoshida H, Obayashi K. Comparative effect of cilnidipine and quinapril on left ventricular mass in mild essential hypertension. *Drugs Exp Clin Res* 2003;29:117–123.
33. Nagai H, Minatoguchi S, Chen XH. Cilnidipine, an N+L-type dihydropyridine Ca channel blocker, suppresses the occurrence of ischemia/reperfusion arrhythmia in a rabbit model of myocardial infarction. *Hypertens Res* 2005;28:361–368.

Nanoparticle-Mediated Delivery of Nuclear Factor κB Decoy Into Lungs Ameliorates Monocrotaline-Induced Pulmonary Arterial Hypertension

Satoshi Kimura, Kensuke Egashira, Ling Chen, Kaku Nakano, Eiko Iwata, Miho Miyagawa, Hiroyuki Tsujimoto, Kaori Hara, Ryuichi Morishita, Katsuo Sueishi, Ryuji Tominaga, Kenji Sunagawa

Abstract—Pulmonary arterial hypertension (PAH) is an intractable disease of the small pulmonary artery that involves multiple inflammatory factors. We hypothesized that a redox-sensitive transcription factor, nuclear factor κB (NF-κB), which regulates important inflammatory cytokines, plays a pivotal role in PAH. We investigated the activity of NF-κB in explanted lungs from patients with PAH and in a rat model of PAH. We also examined a nanotechnology-based therapeutic intervention in the rat model. Immunohistochemistry results indicated that the activity of NF-κB increased in small pulmonary arterial lesions and alveolar macrophages in lungs from patients with PAH compared with lungs from control patients. In a rat model of monocrotaline-induced PAH, single intratracheal instillation of polymeric nanoparticles (NPs) resulted in delivery of NPs into lungs for ≤14 days postinstillation. The NP-mediated NF-κB decoy delivery into lungs prevented monocrotaline-induced NF-κB activation. Blockade of NF-κB by NP-mediated delivery of the NF-κB decoy attenuated inflammation and proliferation and, thus, attenuated the development of PAH and pulmonary arterial remodeling induced by monocrotaline. Treatment with the NF-κB decoy NP 3 weeks after monocrotaline injection improved the survival rate as compared with vehicle administration. In conclusion, these data suggest that NF-κB plays a primary role in the pathogenesis of PAH and, thus, represent a new target for therapeutic intervention in PAH. This nanotechnology platform may be developed as a novel molecular approach for treatment of PAH in the future. (***Hypertension.* 2009;53:877-883.**)

Key Words: pulmonary hypertension ■ lung ■ inflammation ■ leukocytes

Pulmonary arterial hypertension (PAH) is an intractable disease of the small pulmonary arteries that results in a progressive increase in pulmonary vascular resistance, right ventricular failure, and, ultimately, premature death.[1–3] Because its mortality remains high even after the introduction of prostacyclin infusion therapy (which has raised the 5-year survival rate to ≈50%), the development of a more effective and less invasive therapy for PAH is urgently needed.

Recent evidence suggests an important role of monocyte chemoattractant protein (MCP) 1–mediated inflammation in the mechanism of PAH.[4–8] However, the therapeutic benefits of MCP-1 blockade were not optimal for clinical application.[5,6] During the inflammatory process of PAH, several inflammatory factors (eg, MCP-1, interleukin [IL] 1, IL-6, and tumor necrosis factor [TNF] α) are overproduced, leading to a vicious circle.[1–3] A redox-sensitive transcription factor, nuclear factor κB (NF-κB), is known to regulate expression of chemokines such as MCP-1 and multiple inflammatory cytokines such as IL-6 and TNF-α. Blockade of NF-κB by transfection of NF-κB "decoy" oligodeoxynucleotides may attenuate the vascular pathology associated with reduced expression of NF-κB–dependent genes.[9–12] However, no previous study has addressed the specific role of the NF-κB pathway in the pathogenesis of PAH. Therefore, we hypothesized that controlled local delivery of NF-κB decoy into lungs, targeting a battery of multiple important inflammatory cytokines, would be a favorable therapeutic approach for PAH. To this end, we have recently developed bioabsorbable polymeric nanoparticles (NPs) formulated from a poly-(ethylene glycol)-*block*-lactide/glycolide copolymer (PEG-PLGA).[13–15]

The primary aim of this study was to investigate the role of the NF-κB pathway in the pathogenesis of PAH. We first examined the activity of NF-κB in patients with PAH. We then used a rat model of monocrotaline (MCT)-induced PAH to examine whether NP-mediated delivery of the NF-κB decoy can attenuate the development of PAH.

Methods

Histopathologic and Immunohistochemical Examination of Human Lungs

Human lung tissue was obtained from autopsy specimens from 4 patients whose deaths were attributed to idiopathic PAH and 2

Received August 10, 2008; first decision August 26, 2008; revision accepted March 2, 2009.

From the Departments of Surgery (S.K., R.T.), Cardiovascular Medicine (K.E., L.C., K.N., E.I., M.M., K. Sunagawa), and Pathology (K. Sueishi), Graduate School of Medical Science, Kyushu University, Fukuoka; Hosokawa Powder Technology Research Institute (H.T., K.H.), Osaka; and Division of Clinical Gene Therapy (R.M.), Osaka University Medical School, Osaka, Japan.

Correspondence to Kensuke Egashira, Department of Cardiovascular Medicine, Graduate School of Medical Science, Kyushu University, 3-1-1, Maidashi, Higashi-ku, Fukuoka 812-8582, Japan. E-mail egashira@cardiol.med.kyushu-u.ac

Hypertension is available at http://hyper.ahajournals.org DOI: 10.1161/HYPERTENSIONAHA.108.121418

patients whose deaths were attributed to nonlung disease (Figure S1, available in the online data supplement at http://hyper.ahajournals.org). Additional details are provided in the online data supplement.

Preparation of NPs

The NF-κB decoy oligodeoxynucleotides labeled with or without fluorescein-isothiocyanate (FITC) were prepared as described previously.[10,11] The decoy is directed against the NF-κB binding site in the promoter region that corresponds with NF-κB–responsive genes and works to inhibit binding of this transcription factor to the promoter region.[10,11] PEG-PLGA NPs encapsulated with FITC, NF-κB decoy, or FITC-labeled NF-κB decoy were prepared using an emulsion solvent diffusion method.[13,14] The average diameter of PEG-PLGA NPs was 44 nm. To measure FITC release kinetics, FITC-NP was immersed in Tris-EDTA buffer, and the released FITC was measured. Additional details are provided in the online data supplement.

In Vivo Experiments With a Rat Model of MCT-Induced PAH

Rats were SC injected with 60 mg/kg of MCT, which induces severe PAH within 3 weeks.[5,16,17] In the prevention protocol, animals were assigned to either an untreated control group or a group that received a single intratracheal instillation of NF-κB decoy alone (50 μg), FITC-NP (1000 μg of PEG-PLGA), or NF-κB decoy NPs (50 μg of NF-κB decoy per 1000 μg of PEG-PLGA) immediately after MCT (n=6 each). For intratracheal instillation, a volume of 0.1 mL of phosphate buffer suspension of NP or NF-κB decoy was injected gently into the trachea of animals accompanied by an equal volume of air. The biodistribution of FITC in the lung was also examined 3, 7, and 14 days after intratracheal instillation of FITC only, FITC-NPs, or FITC-labeled NF-κB decoy NPs in rats injected with MCT. In the treatment protocol, rats were divided into 2 groups (rats treated with a single intratracheal instillation of phosphate buffer and rats treated with NF-κB decoy NPs; n=33 each) 21 days after MCT injection, when severe PAH had been established.

Hemodynamic Measurements

Three weeks after MCT administration, the animals were anesthetized with sodium pentobarbital, and then polyethylene catheters were inserted into the right ventricle (RV) through the jugular vein and the carotid artery for hemodynamic measurements. RV systolic pressure and systemic blood pressure were measured with a polygraph system (AP-601G, Nihon Kohden).[5]

Assessment of Right Heart Hypertrophy and Pulmonary Arterial Remodeling

After systemic arterial and RV pressure had been recorded, the animals were euthanized, and the lungs and heart were isolated. The RV wall was dissected from the left ventricle (LV) and ventricular septum (S). The wet weight of the RV and LV+S was determined, and RV hypertrophy was expressed as follows: RV/(LV+S).[5]

The lungs were perfused with a solution of 10% phosphate buffered formalin (pH 7.4). At the same time, 10% phosphate buffered formalin (pH 7.4) was administered into the lungs via the tracheal tube at a pressure of 20 cm H_2O. These specimens were processed for light microscopy by routine paraffin embedding. The degree of remodeling (muscularization) of the small peripheral pulmonary arteries was assessed by double immunohistochemical staining of the 3-μm sections with an anti–α-smooth muscle actin antibody (dilution 1:500, clone 1A4, Dako) and anti–platelet endothelial cell adhesion molecule 1 (M-20) antibody (dilution 1:100, Santa Cruz Biotechnology) modified from a protocol described elsewhere.[18]

To assess the type of remodeling in the muscular pulmonary arteries, microscopic images were analyzed. In each rat, 30 to 40 intra-acinar arteries were categorized as muscular (ie, with a complete medial coat of muscle), partially muscular (ie, with only a crescent of muscle), or nonmuscular (ie, with no apparent muscle). The arteries were counted and averaged within a range of diameters from 25 to 50 μm.

Histopathologic and Immunohistochemical Analysis

The degrees of monocyte infiltration were evaluated by immunostaining with the ED-1 (analogue of human CD68) antibody against monocytes. For quantification, a blind observer counted the number of ED-1–positive cells in 10 fields.[4] Monocytes were also subjected to immunostaining with antibodies against FITC, an epitope (α-p65) on the p65 subunit of NF-κB, or nonimmune mouse IgG. The α-p65 monoclonal antibody recognizes an epitope on the p65 subunit that is masked by bound inhibitor of κB (I-κB).[9] Therefore, this antibody exclusively detects activated NF-κB.[12]

Electrophoretic Mobility-Shift Assays

Nuclear extracts were prepared from the whole-lung homogenates using a nuclear extract kit (NE-PER Nuclear and Cytoplasmic Extraction Reagents, Thermo Science) according to the manufacturer's instructions. The protein was measured using a BCA Protein Assay kit (Thermo Science). For NF-κB activation, a nonradioactive electrophoresis mobility-shift assay kit (AY1030, Panomics) was used according to the manufacturer's instructions. Five μg of nuclear protein were incubated for 30 minutes at room temperature with a biotinylated oligonucleotide containing the NF-κB binding site, and then the samples were separated on a nondenaturing polyacrylamide gel and blotted onto a positively charged nylon membrane. After blotting, the oligos on the membrane were fixed using a UV cross-linker oven. Then, the membrane was incubated with streptavidin-horseradish-peroxidase solution at room temperature for 15 minutes and with detection reagents for 5 minutes. Nuclear proteins that were bound to the NF-κB binding site were detected by chemiluminescence with the use of the LAS-1000 detection system (Fujifilm).

Real-Time Quantitative RT-PCR

Real-time PCR amplification was performed with the rat cDNA with the use of the ABI PRI8:21 PM 7000 Sequence Detection System (Applied Biosystems), as described previously.[12] TaqMan primer/probes for MCP-1, TNF-α, IL-1, IL-6, intercellular adhesion molecule 1, and GAPDH, which served as the endogenous reference, were purchased from Applied Biosystems (Assay-on-Demand gene expression products Rn00580555, Rn99999017, Rn00580432, Rn00561420, and Rn00564227 and TaqMan Rodent GAPDH Control Reagents, respectively).

Intracellular Delivery of NPs Incorporated With an FITC-Labeled NF-κB Decoy to Human Monocytes and Pulmonary Arterial Smooth Muscle Cells

The human monocyte cell line THP-1 was obtained from the German Collection of Micro-organisms and Cell Cultures and was used between passages 4 and 8. Cells were cultured in RPMI 1640 with 10% FBS in a humidified atmosphere of 5% CO_2 in air. The cell density was adjusted to 10^6 cells per milliliter in 1 mL of serum-free medium in 35-mm-diameter dishes. The cells were serum deprived 24 hours before the experiment. The growth medium was replaced with FITC-conjugated NF-κB decoy encapsulated PEG-PLGA NP suspension medium (0.5 mg/mL) and then further incubated for 1 hour. At the end of the experiment, the cells were washed 3 times with PBS to eliminate excess NPs that were not incorporated into the cells. Then, the cells were fixed with 10% cold methanol, and nuclei were counterstained with propidium iodide. Cellular uptake of FITC-conjugated NF-κB decoy-encapsulated PEG-PLGA NPs was evaluated by fluorescence microscopy.

Human pulmonary artery smooth muscle cells (PASMCs) were obtained from Cambrex Bio Science, Inc, and cultured as described previously. Cells were used between passages 4 and 8. Human PASMCs were seeded on chambered cover glasses and incubated at 37°C/5% CO_2 until the cells were subconfluent. The following treatments were performed in the same manner.

Lipopolysaccharide-Induced Activation of Human Monocytes

Bacterial lipopolysaccharide (serotype 0111:B4; Sigma) was added at 1 μg/mL to the cells as indicated for each experiment. NF-κB decoy at 5 μg/mL, NF-κB decoy-encapsulated NPs containing 0.1 mg/mL of PEG-PLGA NP and 5 μg/mL of NF-κB decoy, or the vehicle alone was added to the wells simultaneously. Four hours later, the cells were washed 3 times with PBS. NF-κB pathway activity was measured using a TransAM NF-κB p65 ELISA-based assay kit (Active Motif). Nuclear extracts of THP-1 were prepared with the NE-PER kit (Pierce) according to the manufacturer's protocol. All of the procedures were carried out at 4°C. Protein concentration was determined by BCA assay, and 20 μg of protein from each sample were used in the assay. Samples were placed along with 30 μL of binding buffer on a 96-well plate to which oligonucleotides containing an NF-κB consensus binding site had been immobilized. Plates were incubated for 1 hour on a shaker. During this time, the activated NF-κB contained in the sample specifically bound to this nucleotide. The plate was then washed, and the NF-κB complex bound to the oligonucleotides was detected using a primary antibody (100 μL diluted 1:1000 in antibody binding buffer for 1 hour) that is directed against the NF-κB p65 subunit. The plate was then washed again, 100 μL of secondary antibody (diluted 1:1000 in antibody binding buffer) conjugated to horseradish peroxidase was added, and the plate was incubated for 1 hour. The plate was washed again, and 100 μL of developing solution were added. The plate was incubated for 4 minutes away from direct light, 100 μL of stop solution were added, and the plate was read using a plate reader at 450 nm.

Human PASMC Proliferation Assay

Human PASMCs were seeded on 96-well culture plates at 1×10^4 cells per well (n=6 per group) in smooth muscle cells–basal medium with 10% FBS. After 24 hours, the cells were starved for 48 hours in serum-free medium to obtain quiescent nondividing cells. After starvation, 10% FBS was added. Also, a concentration of 1 mg/mL of NF-κB decoy only, NF-κB decoy-encapsulated PEG-PLGA NPs (0.05 mg/mL of PEG-PLGA and 1 mg/mL of decoy), or FITC-encapsulated PEG-PLGA NPs was added to each well. Cells were incubated for another 24 hours after addition of 5′-bromo-2′-deoxyuridine. 5′-Bromo-2′-deoxyuridine incorporation was evaluated by an ELISA kit from Calbiochem.

Statistical Analysis

All of the results are expressed as the mean±SEM. Statistical analysis of differences was performed by ANOVA followed by Bonferroni's multiple comparison test. The survival rates were determined by the Kaplan–Meier method. $P<0.05$ was considered statistically significant.

Results

Activation of NF-κB Expression in Patients With PA6H and in MCT-Induced PAH Rats

Localization of NF-κB activation was examined by immunohistochemical studies in lung tissue from patients using the antibody against α-p65.[9] An intense immunoreactivity of α-p65 was noted primarily in alveolar macrophages and to some extent in small pulmonary arterial lesions (mainly in smooth muscle cells in the medium) from 4 patients with PAH (Figure 1A and Figure S1A). This NF-κB activation was associated with positive staining of MCP-1 and IL-6. In contrast, none at all of α-p65 was detected in 2 control patients whose deaths were not attributed to lung disease (Figure S1B).

In MCT-induced PAH rats, activation NF-κB was noted mainly in alveolar macrophages and weakly in pulmonary artery lesions 7 days after MCT administration (Figure 1B and 1C). An electrophoretic mobility-shift assay was performed to detect the DNA binding activity of NF-κB (Figure S2). The binding activity of the lung increased in rats after MCT injection, which peaked on day 3 and decreased on day 7.

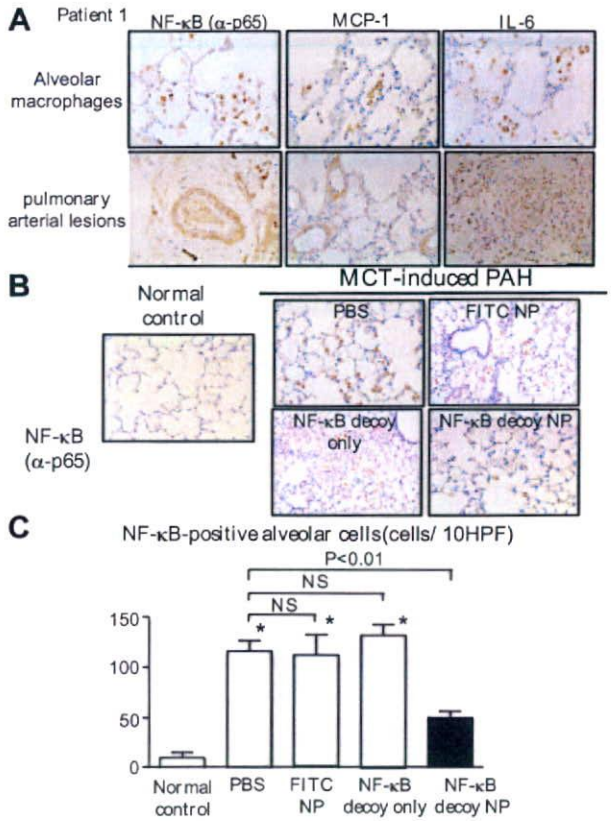

Figure 1. NF-κB activation in patients with PAH and rats with MCT-induced PAH and the effect of intratracheal instillation of NF-κB decoy NPs on NF-κB activation in rats. A, Micrographs of cross sections of the lung from patient 1 stained immunohistochemically with NF-κB (α-p65), MCP-1, and IL-6. Pictures stained with nonimmune IgG control are shown in the inset. Scale bar: 50 μm. B, Micrographs of cross sections of the lung stained immunohistochemically with NF-κB (α-p65) from normal rats and PAH rats 7 days after MCT injection. Scale bar: 50 μm. C, Effects of NF-κB decoy NPs on infiltration of NF-κB (α-p65)–positive cells 7 days after MCT injection. Data are mean±SEM (n=4 each). *$P<0.01$ vs PBS vs normal control.

Effects of Intratracheal Treatment With NF-κB Decoy NP on NF-κB Activation

Single intratracheal instillation of NF-κB decoy NPs, but not FITC NPs or NF-κB decoy only, resulted in marked attenuation of the increased NF-κB (α-p65) activity 7 days after MCT injection (Figure 1B and 1C). Treatment with NF-κB decoy NP markedly attenuated the DNA binding activity of NF-κB after MCT injection (Figure S2).

Because NF-κB was activated in alveolar monocytes and small pulmonary arterial smooth muscle cells in animals and humans with PAH, the effects of NF-κB decoy NPs on NF-κB activity were examined in the human monocyte cell line (THP-1) and in PASMCs in vitro (Figure S3). When those cultured cells were incubated with FITC-labeled NF-κB

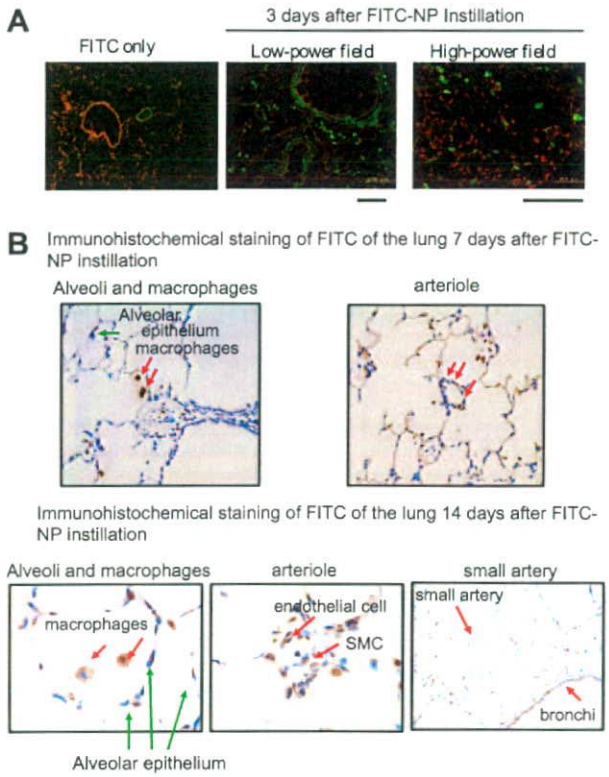

Figure 2. Localization of FITC after FITC-labeled NF-κB decoy NPs postinstillation in the rat lung. A, Fluorescent micrographs of cross sections from lung instillated with FITC only and FITC-labeled NF-κB decoy NPs on day 3 postinstillation. Nuclei were counterstained with propidium iodide (red). Scale bars: 100 μm. B, Micrographs of cross sections stained immunohistochemically against FITC from lung instillated intratracheally with FITC-NPs on days 7 and 14 postinstillation. Scale bars: 100 μm.

decoy NPs for 60 minutes, they were exclusively positive for intracellular localization of FITC. Treatment with NF-κB decoy NPs, but not but with FITC-NPs only or NF-κB decoy only, prevented NF-κB activation in THP-1 cells and attenuated proliferation of human PASMCs.

Localization of FITC-Labeled NF-κB Decoy NPs in the Lung of MCT-Induced PAH

Localization of FITC was examined after a single intratracheal instillation of FITC-labeled NF-κB decoy NPs in animals injected with MCT. Histopathologic examination of lung sections showed that strong FITC signals were detected only in FITC-NP–instillated lung 3 days after instillation, whereas no FITC signals were observed in control noninjected lungs or in lungs injected with FITC only (Figure 2A). There were the FITC-positive cells in bronchi and alveoli, alveolar macrophages, and small arteries. Immunofluorescent staining revealed FITC signals localized mainly in small arteries and arterioles, as well as in small bronchi and alveoli, 7 and 14 days after instillation of FITC-NPs (Figure 2B). FITC signals were not detected in remote organs (liver, spleen, kidney, and heart) on days 1, 3, and 7 (data not shown).

Effects of NF-κB Decoy NP on the Development of PAH in the Rat Model of MCT-Induced PAH

As reported previously by us and by other investigators,[5,16,17] the injection of MCT results in severe PAH (increased RV systolic pressure and RV hypertrophy; Figure 3) associated with small pulmonary arterial remodeling (Figure 4) and increased infiltration of ED-1–positive monocytes (Figure 4) 3 weeks after MCT injection. Single intratracheal treatment with NF-κB decoy NPs but not with NF-κB decoy only or FITC-NPs attenuated the development of PAH (Figure 3), small pulmonary arterial remodeling (Figure 4), and inflammation (Figure 4).

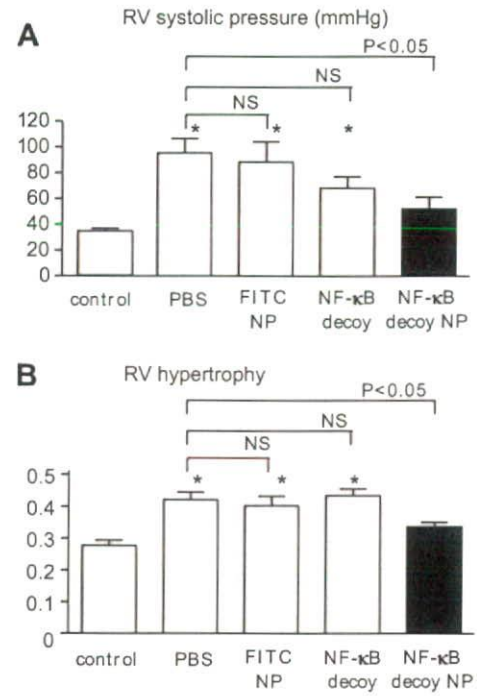

Figure 3. Effects of NF-κB decoy NPs on RV systolic pressure and RV hypertrophy 3 weeks after MCT injection. A, RV systolic pressure 21 days after MCT injection in 4 groups. Data are mean±SEM (n=6 each). *$P<0.05$ vs normal control. B, RV hypertrophy (the ratio of RV/[LV+S]) 21 days after MCT injection in the different treatment groups. Data are mean±SEM (n=6 each). *$P<0.05$ vs normal control.

Effects of NF-κB Decoy NPs on Expression of Proinflammatory Factors

As reported previously,[3,4] MCT-induced PAH was associated with increased gene expression of proinflammatory factors. Treatment with NF-κB decoy NPs significantly reduced the increased gene expression of MCP-1, TNF-α, and IL-1β (Figure 5). NF-κB decoy NPs tended to decrease the expression of IL-6 and intercellular adhesion molecule-1.

In Vitro NP Release Kinetics

An analysis of the in vitro FITC release kinetics from FITC-NP showed an early burst of FITC release such that ≈40% of the total amount ultimately released was present on day 1, followed by sustained release of the remaining FITC over the next 28 days (Figure S4).

Effects of NF-κB Decoy NPs on Survival

Treatment with NF-κB decoy NPs 21 days after MCT injection significantly ($P<0.01$) improved the survival rate (Figure 6).

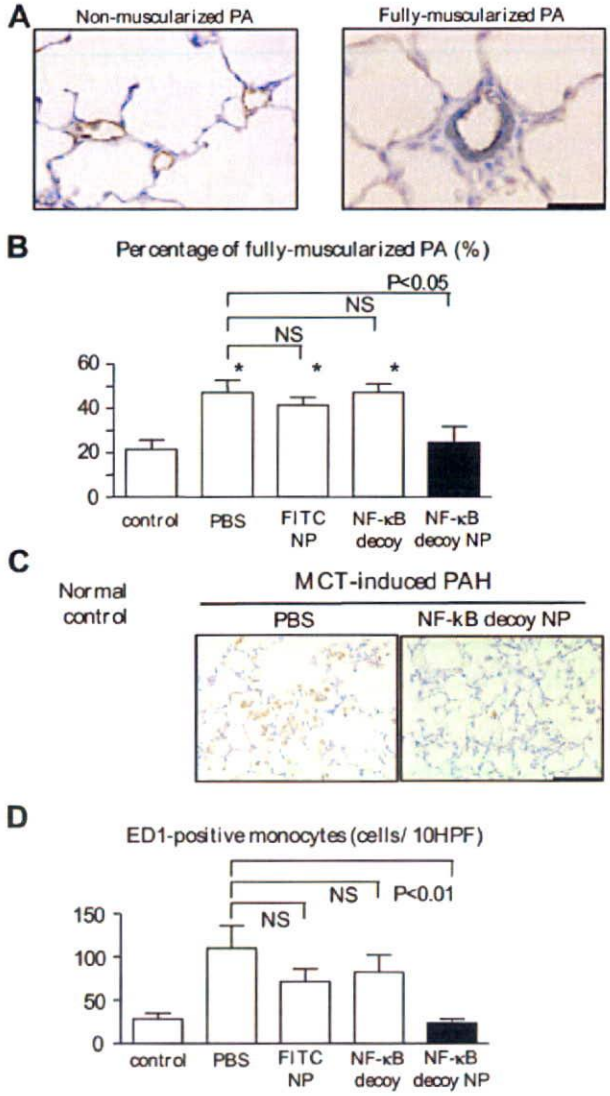

Figure 4. Effects of NF-κB decoy NPs on small pulmonary arterial remodeling and infiltration of monocytes. A, Representative micrographs of nonmuscularized and fully muscularized small pulmonary arteries stained immunohistochemically against the endothelial layer (brown) and medial smooth muscle cells (blue). Scale bar: 50 μm. B, The percentage of fully muscularized small pulmonary arteries in the different treatment groups. Data are mean±SEM (n=6 each). *$P<0.05$ vs normal control. C, Representative micrographs of pulmonary alveoli stained immunohistochemically for ED-1–positive monocytes. Scale bar: 50 μm. D, Infiltration of ED-1–positive monocytes into the lung (the number of positive cells per 10 high-power field cross sections). Data are mean±SEM (n=6 each). *$P<0.01$ vs normal control.

Discussion

The present study demonstrates for the first time that intratracheal instillation of PEG-PLGA NPs is an excellent system for drug delivery of NF-κB decoy to the lung. The FITC signals were detected not only in small bronchial tracts but also in alveolar macrophages and small pulmonary arteries for ≤14 days after a single instillation. After cellular uptake of NPs, NPs might slowly release encapsulated decoy into the cytoplasm as PLGA is hydrolyzed. This might protect the encapsulated decoy from intracellular degradation before its arrival at the nuclear target. Our in vitro studies in cultured human monocytes and pulmonary arterial smooth muscle cells support this notion. Therefore, this platform nanotechnology may represent a novel NP-mediated drug delivery system for treatment of severe lung diseases, including PAH.

The present study also reports a pivotal role of NF-κB in the pathogenesis of PAH. Recently, Sawada et al[19] and Huang et al[20] reported that systemic daily administration of pyrrolidine dithiocarbamate, a nonspecific inhibitor of NF-κB, attenuated the development of MCT-induced PAH. Pyrrolidine dithiocarbamate is known to be a low molecular weight thiol compound and has anti-inflammatory and antioxidant activity independent of the NF-κB pathway. Indeed, in a study by Huang et al,[20] pyrrolidine dithiocarbamate treatment had no effect on MCT-induced NF-κB activation. In contrast, we found in the present study that NF-κB is activated in alveolar macrophages and small pulmonary arteries associated with NF-κB–dependent inflammatory factors (eg, MCP-1, IL-1, and TNF-α) in patients with PAH and rats with MCT-induced PAH, and blockade of NF-κB activation by a single intratracheal instillation of NF-κB decoy NPs reduced inflammatory changes. These data suggest that NF-κB might be pivotal in mediating inflammatory changes seen in PAH.

We also found that intratracheal instillation of NF-κB decoy NPs prevented the development of PAH (increased RV pressure, RV hypertrophy, and pulmonary artery remodeling) in the prevention protocol. We and others have reported that blockade of MCP-1 reduces vascular pathology after vascular injury[9,21–25] and the development of PAH.[5,6] In addition, as we reported in human coronary artery smooth muscle cells in vitro,[12,26] we found that NF-κB decoy NPs attenuated proliferation of human PASMCs in vitro. Therefore, the beneficial effects of NF-κB decoy NPs can be attributable to inhibition of inflammation and smooth muscle cell proliferation resulting from reduced NF-κB activation.

Furthermore, we found that a single intratracheal treatment of NF-κB decoy NPs 3 weeks after MCT injection improved survival rate in the treatment protocol, suggesting that this NP-mediated NF-κB decoy delivery may have significant therapeutic effects. We did not examine the therapeutic effects of repetitive intratracheal instillation of NF-κB decoy NPs, because it is technically difficult to perform multiple intratracheal instillation of this NP system in rats and other small animals. For translation of our present findings into clinical medicine, further studies are needed to investigate whether repetitive delivery of NPs into lungs produces greater therapeutic effects over time.

Several points are worth mentioning with regard to potential clinical applicability. First, from a toxicological point of view, no adverse reactions, eg, pulmonary inflammation, after exposure to a single intratracheal instillation of FITC-NPs (PEG-PLGA at 1 mg per body) or NF-κB decoy NPs (NF-κB decoy at 50 μg per body in rats weighing 250 to 300 g) were noted in the rat model, suggesting that the NPs used in this study may not cause an adverse reaction. However, the 3-week observation period for this NP system might be too short to determine its safety. Second, we reported recently that neither intravenous injection of the NF-κB decoy at 1 mg per body in monkeys nor deployment

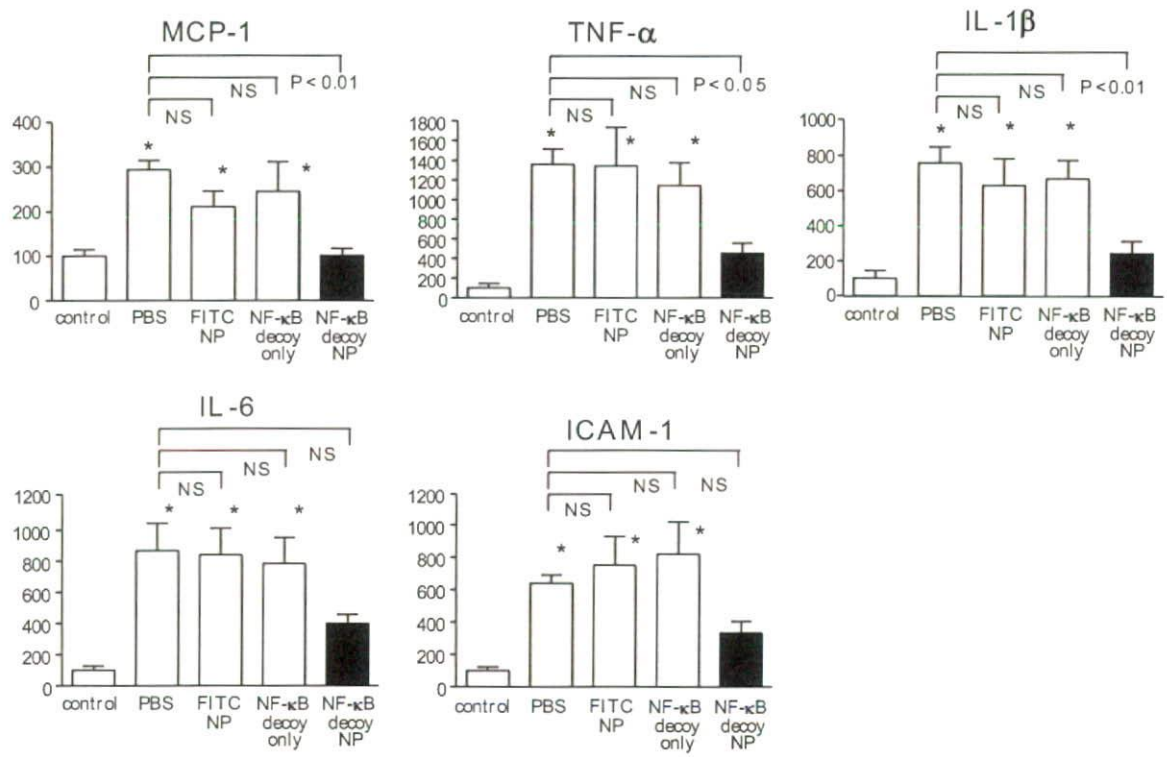

Figure 5. Effects of NF-κB decoy NPs on mRNA levels of various inflammatory and proliferative factors 21 days after MCT injection (n=5 each). *$P<0.01$ vs normal control.

of an NF-κB decoy-eluting stent (≈600 μg per stent) in rabbits showed systemic adverse effects.[12] More important are the findings of a clinical trial that we completed recently to test the feasibility and safety of the NF-κB decoy. The decoy was transfected into the stented coronary artery sites at doses of 1000, 2000, or 4000 μg per body via a channel balloon catheter immediately after successful percutaneous coronary intervention in 18 patients with flow-limiting coronary stenosis.[27] The patients showed low restenosis rates and no evidence of systemic adverse effects during the 6-month observation period. These data support the notion that NF-κB decoy can be applied in a clinical setting. Third, this NP system itself is not suitable for inhalant therapy, because it is known that most inhaled NPs are exhaled rather than being delivered into the lung.[28] In contrast, microparticles with aerodynamic diameters between 2 and 8 μm reach small bronchi. However, the microparticles are easily recognized and eliminated by the mucociliary clearance system and alveolar macrophages immediately after they reach the small bronchi.[28] In contrast, polymeric NPs escape the clearance system of the lung when they are delivered into small bronchi and are, thus, taken up by alveoli, macrophages, and pulmonary small vessels. Therefore, to use this NP system for inhalant therapy, we need to develop the nanocomposite microsized particles[28] that will decompose to NPs after reaching the small bronchi.

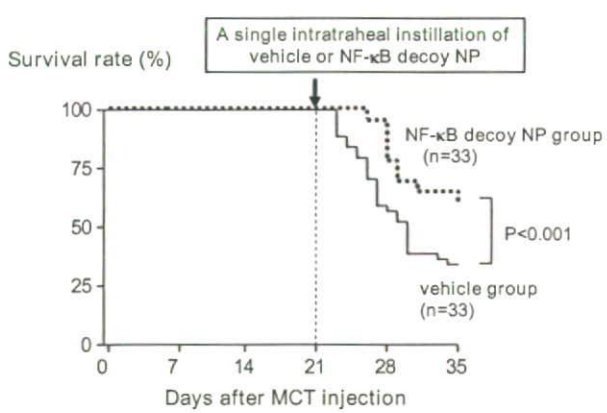

Figure 6. Effects of NF-κB decoy NPs on survival rate. Survival rate analyzed by the Kaplan–Meier method in vehicle and NF-κB decoy NP groups.

Perspectives

This study has shown that NF-κB is activated in pulmonary arterial lesions in patients with PAH and in rats with MCT-induced PAH, and blockade of NF-κB by NP-mediated NF-κB decoy delivery not only prevented the development of MCT-induced PAH in the prevention protocol but also improved survival rate in the treatment protocol. These data support the notion that NF-κB plays a pivotal role in the pathogenesis of PAH and, thus, represents a new therapeutic target for PAH. This nanotechnology platform may be developed as a more effective and less invasive nanomedicine in PAH therapy.

Sources of Funding

This study was supported by Grants-in-Aid for Scientific Research (19390216 and 19650134) from the Ministry of Education, Science, and Culture (Tokyo, Japan) and by Health Science Research grants

(Research on Translational Research and Nano-medicine) from the Ministry of Health, Labor, and Welfare (Tokyo, Japan).

Disclosures

K.E. and R.M. hold a patent on the results reported in this study. The remaining authors report no conflicts.

References

1. Farber HW, Loscalzo J. Pulmonary arterial hypertension. *N Engl J Med*. 2004;351:1655–1665.
2. Humbert M, Sitbon O, Simonneau G. Treatment of pulmonary arterial hypertension. *N Engl J Med*. 2004;351:1425–1436.
3. Stenmark KR, Fagan KA, Frid MG. Hypoxia-induced pulmonary vascular remodeling: cellular and molecular mechanisms. *Circ Res*. 2006; 99:675–691.
4. Sanchez O, Marcos E, Perros F, Fadel E, Tu L, Humbert M, Dartevelle P, Simonneau G, Adnot S, Eddahibi S. Role of endothelium-derived CC chemokine ligand 2 in idiopathic pulmonary arterial hypertension. *Am J Respir Crit Care Med*. 2007;176:1041–1047.
5. Ikeda Y, Yonemitsu Y, Kataoka C, Kitamoto S, Yamaoka T, Nishida K, Takeshita A, Egashira K, Sueishi K. Anti-monocyte chemoattractant protein-1 gene therapy attenuates pulmonary hypertension in rats. *Am J Physiol Heart Circ Physiol*. 2002;283:H2021–H2028.
6. Kimura H, Kasahara Y, Kurosu K, Sugito K, Takiguchi Y, Terai M, Mikata A, Natsume M, Mukaida N, Matsushima K, Kuriyama T. Alleviation of monocrotaline-induced pulmonary hypertension by antibodies to monocyte chemotactic and activating factor/monocyte chemoattractant protein-1. *Lab Invest*. 1998;78:571–581.
7. Katsushi H, Kazufumi N, Hideki F, Katsumasa M, Hiroshi M, Kengo K, Hiroshi D, Nobuyoshi S, Tetsuro E, Hiromi M, Tohru O. Epoprostenol therapy decreases elevated circulating levels of monocyte chemoattractant protein-1 in patients with primary pulmonary hypertension. *Circ J*. 2004;68:227–231.
8. Itoh T, Nagaya N, Ishibashi-Ueda H, Kyotani S, Oya H, Sakamaki F, Kimura H, Nakanishi N. Increased plasma monocyte chemoattractant protein-1 level in idiopathic pulmonary arterial hypertension. *Respirology*. 2006;11:158–163.
9. Brand K, Page S, Rogler G, Bartsch A, Brandl R, Knuechel R, Page M, Kaltschmidt C, Baeuerle PA, Neumeier D. Activated transcription factor nuclear factor-kappa B is present in the atherosclerotic lesion. *J Clin Invest*. 1996;97:1715–1722.
10. Morishita R, Higaki J, Tomita N, Ogihara T. Application of transcription factor "decoy" strategy as means of gene therapy and study of gene expression in cardiovascular disease. *Circ Res*. 1998;82:1023–1028.
11. Kitamoto S, Egashira K, Kataoka C, Koyanagi M, Katoh M, Shimokawa H, Morishita R, Kaneda Y, Sueishi K, Takeshita A. Increased activity of nuclear factor-kappaB participates in cardiovascular remodeling induced by chronic inhibition of nitric oxide synthesis in rats. *Circulation*. 2000; 102:806–812.
12. Ohtani K, Egashira K, Nakano K, Zhao G, Funakoshi K, Ihara Y, Kimura S, Tominaga R, Morishita R, Sunagawa K. Stent-based local delivery of nuclear factor-kappaB decoy attenuates in-stent restenosis in hypercholesterolemic rabbits. *Circulation*. 2006;114:2773–2779.
13. Murakami H, Kobayashi M, Takeuchi H, Kawashima Y. Preparation of poly(DL-lactide-co-glycolide) nanoparticles by modified spontaneous emulsification solvent diffusion method. *Int J Pharm*. 1999;187:143–152.
14. Kawashima Y, Yamamoto H, Takeuchi H, Hino T, Niwa T. Properties of a peptide containing DL-lactide/glycolide copolymer nanospheres prepared by novel emulsion solvent diffusion methods. *Eur J Pharm Biopharm*. 1998;45:41–48.
15. Panyam J, Zhou WZ, Prabha S, Sahoo SK, Labhasetwar V. Rapid endolysosomal escape of poly(DL-lactide-co-glycolide) nanoparticles: implications for drug and gene delivery. *FASEB J*. 2002;16:1217–1226.
16. Schermuly RT, Dony E, Ghofrani HA, Pullamsetti S, Savai R, Roth M, Sydykov A, Lai YJ, Weissmann N, Seeger W, Grimminger F. Reversal of experimental pulmonary hypertension by PDGF inhibition. *J Clin Invest*. 2005;115:2811–2821.
17. Cowan KN, Heilbut A, Humpl T, Lam C, Ito S, Rabinovitch M. Complete reversal of fatal pulmonary hypertension in rats by a serine elastase inhibitor. *Nat Med*. 2000;6:698–702.
18. Quinlan TR, Li D, Laubach VE, Shesely EG, Zhou N, Johns RA. eNOS-deficient mice show reduced pulmonary vascular proliferation and remodeling to chronic hypoxia. *Am J Physiol Lung Cell Mol Physiol*. 2000;279:L641–L650.
19. Sawada H, Mitani Y, Maruyama J, Jiang BH, Ikeyama Y, Dida FA, Yamamoto H, Imanaka-Yoshida K, Shimpo H, Mizoguchi A, Maruyama K, Komada Y. A nuclear factor-kappaB inhibitor pyrrolidine dithiocarbamate ameliorates pulmonary hypertension in rats. *Chest*. 2007;132: 1265–1274.
20. Huang J, Kaminski PM, Edwards JG, Yeh A, Wolin MS, Frishman WH, Gewitz MH, Mathew R. Pyrrolidine dithiocarbamate restores endothelial cell membrane integrity and attenuates monocrotaline-induced pulmonary artery hypertension. *Am J Physiol Lung Cell Mol Physiol*. 2008;294: L1250–L1259.
21. Egashira K. Molecular mechanisms mediating inflammation in vascular disease: special reference to monocyte chemoattractant protein-1. *Hypertension*. 2003;41:834–841.
22. Egashira K. Clinical importance of endothelial function in arteriosclerosis and ischemic heart disease. *Circ J*. 2002;66:529–533.
23. Ohtani K, Usui M, Nakano K, Kohjimoto Y, Kitajima S, Hirouchi Y, Li XH, Kitamoto S, Takeshita A, Egashira K. Antimonocyte chemoattractant protein-1 gene therapy reduces experimental in-stent restenosis in hypercholesterolemic rabbits and monkeys. *Gene Ther*. 2004;11: 1273–1282.
24. Usui M, Egashira K, Ohtani K, Kataoka C, Ishibashi M, Hiasa K, Katoh M, Zhao Q, Kitamoto S, Takeshita A. Anti-monocyte chemoattractant protein-1 gene therapy inhibits restenotic changes (neointimal hyperplasia) after balloon injury in rats and monkeys. *FASEB J*. 2002;16: 1838–1840.
25. Egashira K, Zhao Q, Kataoka C, Ohtani K, Usui M, Charo IF, Nishida K, Inoue S, Katoh M, Ichiki T, Takeshita A. Importance of monocyte chemoattractant protein-1 pathway in neointimal hyperplasia after periarterial injury in mice and monkeys. *Circ Res*. 2002;90:1167–1172.
26. Lemarie CA, Esposito B, Tedgui A, Lehoux S. Pressure-induced vascular activation of nuclear factor-kappaB: role in cell survival. *Circ Res*. 2003; 93:207–212.
27. Egashira K, Suzuki J, Ito H, Aoki M, Isobe M, Morishita R. Long-term follow up of initial clinical cases with NF-kappaB decoy oligodeoxynucleotide transfection at the site of coronary stenting. *J Gene Med*. 2008; 10:805–809.
28. Tomoda K, Ohkoshi T, Kawai Y, Nishiwaki M, Nakajima T, Makino K. Preparation and properties of inhalable nanocomposite particles: effects of the temperature at a spray-dryer inlet upon the properties of particles. *Colloids Surf B Biointerfaces*. 2008;61:138–144.

Acquisition of Brain Na Sensitivity Contributes to Salt-Induced Sympathoexcitation and Cardiac Dysfunction in Mice With Pressure Overload

Koji Ito, Yoshitaka Hirooka, Kenji Sunagawa

Abstract—In animal models of salt-sensitive hypertension, high salt augments sympathetic outflow via central mechanisms. It is not known, however, whether pressure overload affects salt sensitivity, thereby modifying central sympathetic outflow and cardiac function. We induced left ventricular hypertrophy with aortic banding in mice. Four weeks after aortic banding (AB-4), the left ventricle wall thickness was increased without changing the percentage fractional shortening. AB-4 mice were then fed either a high-salt (8%) diet or regular-salt diet for additional 4 weeks. Cardiac dysfunction, wall thickness, and 24-hour urinary catecholamine excretion were increased with high-salt diet compared with regular-salt diet. We then examined brain Na sensitivity. Intracerebroventricular infusion of high-Na (0.2 mol/L) artificial cerebrospinal fluid into AB-4 mice and mice Sham-4 increased urinary catecholamine excretion, arterial pressure, and heart rate more in AB-4 mice than in Sham-4 mice. Intracerebroventricular infusion of an epithelial Na channel blocker (benzamil) into mice with high-salt diet significantly decreased urinary catecholamine excretion and improved cardiac function. Infusion of either an angiotensin II type 1 receptor blocker or a Rho-kinase inhibitor also attenuated the salt-induced sympathetic hyperactivation and cardiac dysfunction in mice with high-salt diet. The levels of angiotensin II type 1 receptor and phosphorylated moesin, a substrate of Rho-kinase, were significantly greater in AB-4 mice than in Sham-4 mice. These results suggest that mice with pressure overload acquire brain Na sensitivity because of the activation of epithelial Na channel via Rho-kinase and angiotensin II, and this mechanism contributes to salt-induced sympathetic hyperactivation, further pressure overload, and cardiac dysfunction. (*Circ Res*. **2009;104:1004-1011.**)

Key Words: hypertension ■ heart failure ■ hypertrophy ■ sympathetic nervous system ■ brain ■ sodium chloride

As an environmental factor, high salt intake increases sympathetic activity in genetic models of hypertension.[1–3] In these salt-sensitive hypertensive rats, central mechanisms, such as enhanced Na sensitivity, as well as renal mechanisms contribute to high salt–induced sympathetic activation and arterial pressure elevation.[1–3] Enhanced central sympathetic outflow is also observed in animal models of heart failure,[4–7] and intracerebroventricular (ICV) infusion of an amiloride analog, benzamil, which inhibits the epithelium Na^+ channels (ENaCs), may reduce the enhanced sympathetic drive and improve cardiac function in rats with myocardial infarction.[4]

The effects of sustained cardiac pressure overload on cardiac function and/or cardiac muscles have been investigated using aortic banding models.[8,9] It is not known whether the sustained cardiac pressure overload without a genetic predisposition to salt sensitivity influences brain Na sensitivity. Furthermore, few studies have examined the relationship between central sympathetic outflow and cardiac function in animals with pressure overload. Therefore, the aim of the present study was to determine whether a sustained pressure overload produced in mice without a genetic predisposition to salt sensitivity induces brain Na sensitivity, thereby enhancing the central sympathetic outflow leading to cardiac dysfunction. For this purpose, we examined the effects of high salt intake on brain Na concentration, sympathetic activity, arterial pressure, and cardiac function in mice with pressure overload produced by aortic banding. To elucidate brain Na sensitivity, we infused high-Na artificial cerebrospinal fluid (aCSF) ICV in mice with or without pressure overload induced by aortic banding and evaluated sympathetic activity and arterial pressure. In addition, to determine whether brain Na sensitivity is acquired in this model, we examined the effects of the ENaC blocker benzamil[4,5] on high salt–induced activation of the sympathetic nervous system and arterial pressure elevation, because ENaCs on the blood side of the choroidal epithelium may have an important role in Na transport into the CSF, as well as Na^+-K^+ ATPase on the CSF side of choroidal epithelium.[3,10,11] In addition, to explore the mechanisms involved, we also evaluated the role of brain

Original received October 7, 2008; revision received March 5, 2009; accepted March 10, 2009.
From the Department of Cardiovascular Medicine, Kyushu University Graduate School of Medical Sciences, Fukuoka, Japan.
Correspondence to Yoshitaka Hirooka, MD, PhD, FAHA, Department of Cardiovascular Medicine, Kyushu University Graduate School of Medical Sciences, 3-1-1, Higashi-ku, Fukuoka 812-8582, Japan. E-mail hyoshi@cardiol.med.kyushu-u.ac.jp

Circulation Research **is available at http://circres.ahajournals.org** **DOI: 10.1161/CIRCRESAHA.108.188995**

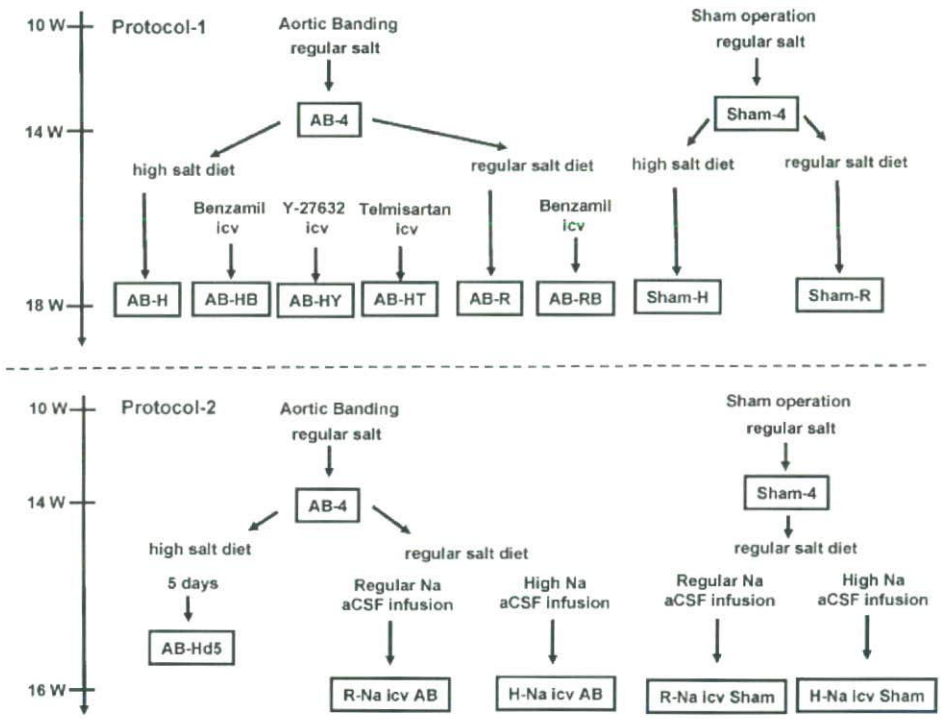

Figure 1. Experimental protocol and time line. W indicates weeks.

ENaCs in the enhanced sympathetic activity and cardiac dysfunction induced by high salt intake in mice with pressure overload and the relationship of brain ENaCs to the Rho/Rho-kinase pathway and the renin–angiotensin system (RAS) in the brain, because ENaCs in kidney are reported to be activated by the Rho/Rho-kinase pathway[12] and RAS.[13]

Materials and Methods

Animals

The study was reviewed and approved by the Committee on Ethics of Animal Experiments, Kyushu University Graduate School of Medical Sciences, and conducted according to the Guidelines for Animal Experiments of Kyushu University. Male Institute of Cancer Research (ICR) mice (10 weeks old; SLC, Fukuoka, Japan) were used.

Mouse Pressure Overload Model Preparation

The suprarenal abdominal aorta was banded in ICR mice (AB mice) to create the pressure overload model[14] or sham operation (Sham mice) as a control. We divided these mice into the groups represented in Figure 1. For details, see the online data supplement, available at http://circres.ahajournals.org.

Evaluation of Cardiac Function

Cardiac function was evaluated by echocardiography.[15,16] Serial M-mode echocardiography was performed under light sodium pentobarbital anesthesia with spontaneous respiration. Cardiac function was also evaluated by the left ventricular end-diastolic pressure (LVEDP). A conductance catheter (1.4 Fr; Miller Instruments) was inserted into the right carotid artery and advanced across the aortic valve into the left ventricle. See the online data supplement for details.

Measurement of Arterial Pressure and Heart Rate

Under sodium pentobarbital anesthesia and mechanical ventilation, a catheter was inserted into the right carotid artery and arterial pressure and heart rate were measured. In another protocol, we also measured arterial pressure and heart rate in awake AB mice fed a high-salt diet (AB-H) and AB mice fed with a regular salt diet (AB-R) using a radiotelemetry system implanted in the left carotid artery.[17] See the online data supplement for details.

Evaluation of Sympathetic Activity

Sympathetic activity was evaluated by measuring 24-hour urinary norepinephrine (U-NE) and urinary epinephrine (U-E) excretion using high-performance liquid chromatography.[15,18]

Evaluation of Na Sensitivity

We evaluated U-NE, U-E, arterial pressure, and heart rate responses to a high-salt diet or high-Na aCSF (0.2 mol/L, 1 μL/min for 10 minutes) ICV infusion in each group. In addition, we measured Na concentrations in the brain tissue (circumventricular tissues including the hypothalamus) of mice in each group. Furthermore, to examine the response of other central stimuli, we performed ICV infusion of angiotensin II (0.5 nmol/L, 1 μL/min for 5 minutes) and carbachol (0.1 mmol/L, 1 μL/min for 5 minutes). See the online data supplement for details.

Measurement of Organ Weight

After completion of the experiments, mice were killed with an overdose of sodium pentobarbital, and the heart and lungs were removed and weighed.

Measurement of Serum Parameters

We measured the serum concentrations of sodium, creatinine, and aldosterone in each group. See the online data supplement for details.

Evaluation of the Effects of Na Channel Blockade in the Brain

To assess the effects of Na channel blockade in the brain, benzamil, a specific ENaC blocker, was infused ICV (1 mg/ml, 0.11 μL/h for 28 days[14]). The U-NE and U-E excretion, arterial pressure, heart rate, and organ weight were measured, and echocardiography was per-